On Channel Allocation of Directional Wireless Networks Using Multiple Channels

Hong-Ning Dai*, Hao Wang† and Hong Xiao‡
*Macau University of Science and Technology, Macau SAR
hndai@ieee.org
†Norwegian University of Science and Technology, Aalesund, Norway
hawa@hials.no
‡Faculty of Computer, Guangdong University of Technology, Guangzhou, China
wh_red@gdut.edu.cn

***Abstract*— This paper investigates the channel allocation problem in multi-channel wireless networks with directional antennas. In particular, we propose a general analytical framework on the number of channels, in which we consider a new directional antenna model. This antenna model is more general than existing antenna models since other existing antenna models can be regarded as a special case of our model. Besides, it can accurately depict directional antenna with consideration of side-lobes and back-lobes. Moreover, we derive the upper bounds on the number of channels of such networks to ensure collision-free communications. Our results are also insightful to the network design and network deployment.**

***Index Terms*— Directional Communications; Wireless Networks; Multiple Channels**

I. Introduction

The proliferation of wireless networks as well as various wireless services is driving the new demands on the precious wireless spectrum result. Therefore, how to use wireless spectrum efficiently has received extensive attentions recently. One of current solutions to improve the network performance is to use multiple channels instead of using a single channel in wireless networks. Both the experimental results and the theoretical results [1]–[5] show that using multiple channels can significantly improve the network throughput due to the improved spectrum reuse. However, most of the studies assume that each node is equipped with omni-directional antennas only, which can cause higher interference and result in poor spectrum reuse. We call such multi-channel wireless networks with omni-directional antennas as OMN-Nets.

Recent studies such as [6]–[9] found that using directional antennas instead of omni-directional antennas in wireless networks can greatly improve the network throughput. In contrast to omni-directional antennas, directional antennas can concentrate the radio signal to some directions so that the interference to other undesired directions can be reduced. As a result, the spectrum reuse can be further improved and can consequently enhance the network performance. The integration of directional antennas and multiple channels can potentially improve the network performance further. Some of most recent works such as [10], [11] found that using directional antennas in multi-channel wireless networks can improve the capacity and connectivity. We call such multi-channel wireless networks with directional antennas as DIR-Nets.

However, there are few works on the channel allocation problem with DIR-Nets. Although [12] investigated the channel allocation problem with DIR-Nets, this work only considers an idealistic directional antenna model without consideration of side-lobes and back-lobes of antennas, which can potentially affect the network performance [13]. In this paper, we establish a general analytical framework on the channel allocation problem with DIR-Nets, in which we consider a new antenna model - Iris. This new antenna model is more general than existing antenna models and can accurately model directional antenna with consideration of side-lobes and back-lobes. We also derive the upper bounds on the number of channels in DIR-Nets.

The rest of this paper is organized as follows. Section II presents the antenna models. We then give the system models in Section III. Section IV next derives the upper bounds on the number of channels to ensure collision-free communications in DIR-Nets. Finally, we conclude the paper in Section V.

II. Antenna Models

A. Directional Antennas

An antenna is a device that is used for radiating/collecting radio signals into/from space. An omni-directional antenna, which can radiate/collect radio signals uniformly in all directions in space, is typically used in conventional wireless networks. Different from an omni-directional antenna, a directional antenna can concentrate transmitting or receiving capability to some desired directions so that it has better performance than an omni-directional antenna.

To model the transmitting or receiving capability of an antenna, we often use the *antenna gain*, which is the directivity of an antenna in 3-D space. The antenna gain of an antenna can be expressed in *radiation pattern* in 3-D space as the following equation [13],

$$G(\vec{d}) = \eta \frac{U(\vec{d})}{U_{ave}} \quad (1)$$

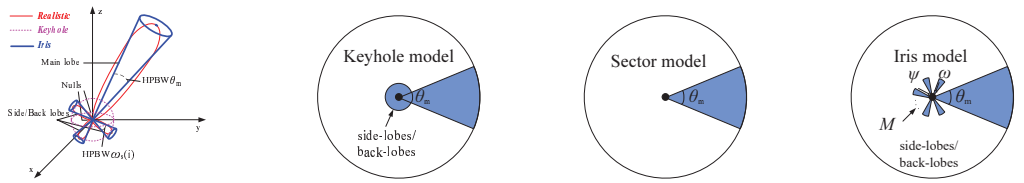

(a) Antenna models in 3D space (b) Keyhole model (c) Sector model (d) Iris model

Fig. 1. Directional Antenna Models

where $U(\vec{d})$ is the power density in the direction $\vec{d}$, which is denoted by a vector, U_{ave} is the average power density over all directions and η is the efficiency factor, which is set to be 1 since an antenna is often assumed to be lossless.

It is obvious that an omni-directional antenna has the gain $G_o = 1$ (or 0 dBi) since it radiates the radio signal uniformly in all directions. Different from an omni-directional antenna, a directional antenna can radiate or receive radio signals more effectively in some directions than in others. A directional antenna consists of the *main-lobe* (or *main-beam*) with the largest *radiation intensity* and the *side-lobes* and *back-lobes* with the smaller radiation intensity. A typical antenna radiation pattern of a Uniform Circle Array (UCA) in 3-D space is shown in Fig. 1(a).

To accurately depict a directional antenna, we introduce the following properties:

- *Main beam* (main lobe) is the radiation *lobe* with the *maximum* antenna gain.
- *Half Power Beam Width* (*HPBW*) is the angular width between the half-power (-3 dB) points of the main lobe.
- *Side/Back lobes* are the radiation lobes with *maximal* antenna gain (i.e., the local maximal values).
- *Nulling capability* is the capability of a directional antenna employing *nulls* to counteract unwanted interference in some undesired directions.

B. Simplified Directional Antenna Models

It is complicated to compute the antenna gain of a realistic antenna in each direction. Besides, realistic antenna model can not be used to solve the problem of deriving the optimal bounds on the network connectivity [14]. Thus, several simplified directional antenna models have been proposed. In particular, an approximated antenna model has been proposed in [15] and been widely used in [6], [14]. This model is named as *Keyhole* antenna model due to the geometrical analogy to the archaic keyhole in 2-D plane. As shown in Fig. 1(a), Keyhole model consists of one main beam with *beamwidth* θ_m (equal to the HPBW θ_m of a realistic antenna) and side/back lobes approximated by a sphere (the dash line). We next derive the antenna gain of Keyhole model in 2-D plane.

As shown in Fig. 1(b), Keyhole model consists one main-lobe (a sector) with beamwidth θ_m and side-lobes back-lobes denoted by a circle. Since the sum of the radiated power in each direction of an antenna is equal to the radiation power P [13], we have

$$G_m(\vec{d}) \cdot U_{ave} \cdot \theta_m + G_s(\vec{d}) \cdot U_{ave} \cdot (2\pi - \theta_m) = P \quad (2)$$

where $G_s(\vec{d})$ denotes the gain of the back-lobes and the side-lobes and $P = 2\pi \cdot U_{ave}$.

Then, we have

$$G_m = \frac{2\pi - G_s \cdot (2\pi - \theta_m)}{\theta_m} \quad (3)$$

$$G_s = \frac{2\pi - G_m \cdot \theta_m}{2\pi - \theta_m}, \quad (4)$$

where we ignore the vector notation $\vec{d}$ in G_m and G_s for simplicity since they are uniform within θ_m and $2\pi - \theta_m$, respectively.

Sector model [10], [16] is another simplified directional antenna model, which can be regarded as a special case of Keyhole model. As shown in Fig. 1(c), Sector model consists only one main lobe and all the side/back lobes are ignored, i.e., $G_s = 0$. Therefore, we have

$$G_m = \frac{2\pi}{\theta_m}. \quad (5)$$

C. Iris Antenna Model

Either Sector antenna model or Keyhole antenna model somehow over-simplify the radiation pattern of a realistic directional antenna. For example, the sector model may "over-estimate" the performance since it ignores the side-lobes and the back-lobes, which however significantly affect the network performance [17]. The keyhole model may "under-estimate" the performance since it regards all the side-lobes and back-lobes as a circle and ignores the nulling capability of an antenna [7], which somehow can cancel the interference to other nodes.

To overcome the limitations of existing antenna models such as Keyhole and Sector models, we propose a new directional antenna model to approximate the radiation pattern of realistic antennas. Our model consists of one sectoral main beam and several sectoral side/back lobes. We name this model as *Iris model* since it is geometrically analogous to an Iris flower. Fig. 1(a) shows our Iris model, in which the sectoral main beam is analogous to the petal of Iris flower and the sectoral side/back lobes are analogous to the sepals of the flower. We then derive the antenna gain of Iris model in 2-D plane as follows.

For simplicity, each side-lobe is regarded to be identical and is uniformly distributed in $2\pi - \theta_m$ (the separation angle between any two adjacent lobes are ψ) as shown in Fig. 1(d).

We denote the number of side-lobes by M, which depends on the number of side/back-lobes in realistic antennas. There is a constraint on the number of side-lobes M, the angle of each lobe ω and the separation angle ψ, which are denoted as the following equation

$$\theta_m + M \cdot \omega + (M+1) \cdot \psi = 2\pi \tag{6}$$

Similarly, we can calculate the gain of the main-lobe and the gain of each side/back-lobes. First, we have

$$G_m \cdot U_{ave} \cdot \theta_m + M \cdot G_s(\vec{d}) \cdot U_{ave} \cdot (2\pi - \theta_m) = P \tag{7}$$

where $P = 2\pi \cdot U_{ave}$.

We then have

$$G_m = \frac{2\pi - M \cdot G_s \cdot (2\pi - \theta_m)}{\theta_m} \tag{8}$$

$$G_s = \frac{1}{M} \cdot \frac{2\pi - G_m \cdot \theta_m}{2\pi - \theta_m} \tag{9}$$

Generality of Iris model: Our proposed Iris model is more general than existing antenna models. In particular, other antenna models such as Sector model, Keyhole model and omni-directional model can be regarded as special cases of our Iris model under the following scenarios.

(1) Keyhole model is a special case of our Iris model: When $M = 1$ and $\theta_m = 0$, there is only one side-lobe, which is a circle with angle $2\pi - \omega$. In this configuration, our model becomes Keyhole model and G_m and G_s in Eq. (8) and Eq. (9) are consistent with those in Eq. (3) and Eq. (4), respectively.

(2) Sector model is a special case of our Iris model: When $M = 0$, there is no side/back-lobes and our model becomes the sector model. The main antenna gain $G_m = \frac{2\pi}{\theta_m}$, which is consisted with Eq. (5) in the sector model.

(3) Omni-directional model is a special case of our Iris model: When $M = 0$ and $\psi = 0$, $\theta_m = 2\pi$, our model becomes the omni-directional model and $G_m = G_o = 1$.

III. System Models

A. Interference Model

We propose an interference model to analyze DIR-Nets. Our model only considers directional transmission and directional reception, which can maximize the benefits of directional antennas.

Two nodes X_i and X_j can establish a bi-directional *link* denoted by l_{ij} if and only if the following conditions are satisfied.

(1) X_j is within the *transmission range* of X_i and X_i is within the *transmission range* of X_j.
(2) X_j is covered by the antenna beam of X_i. Similarly, X_i is also covered by the antenna beam of X_j.
(3) No other node within the *interference range*(the interference range is used to denote the maximum distance within which a node can be interfered by an interfering signal) is simultaneously transmitting over the same channel and in the same direction toward X_j.

We call two nodes in *conflict* with each other if they are located within the interference range of each other and their antenna beams are pointed toward each other. For example, in Figure 2, node X_k within the interference range of node X_j may conflict with X_j. Link l_{ij} *conflicts* with link l_{kl} if either node of one link conflicts with either node of the other link.

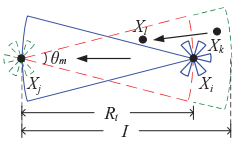

Fig. 2. The Interference Model.

We next analyze the interference range.

B. Interference Range

We denote the node whose transmission causes the interference to other nodes as the *interfering* node. The node whose reception is interfered by other *interfering* nodes is denoted as *interfered* node.

We assume that the interfering node transmits with power P. The received power at the interfered node at a distance d from the interfering node is denoted by P_r, which can be calculated by

$$P_r = C_1 G_t G_r P \frac{1}{d^\alpha}, \tag{10}$$

where C_1 is a constant, G_t and G_r denote the antenna gain of the interfering node and the antenna gain of the interfered node, respectively, and α is the path loss factor usually ranging from 3 to 5 [18].

When an interfering node interferes with an interfered node, the received power at the interfered node P_r is required to be no less than a threshold P_0, *i.e.*, $P_r \geq P_0$. We then have

$$P_0 = C_1 G_t G_r P_t \frac{1}{I^\alpha}, \tag{11}$$

where I is defined as the *interfering range*.

Solving this equation, we have

$$I = \left(\frac{C_1 G_t G_r P_t}{P_0}\right)^{\frac{1}{\alpha}}. \tag{12}$$

Eq. (13) is a general expression of the interference range for both OMN-Nets and DIR-Nets. With regard to an OMN-Net, the interference range denoted by I_o can be trivially calculated as follows,

$$I_o = \left(\frac{C_1 P_t}{P_0}\right)^{\frac{1}{\alpha}}, \tag{13}$$

where $G_t = G_r = G_o = 1$ as shown in Section II.

TABLE I
Four scenarios.

Scenarios	*Interfering node*	*Interfered node*	*Interference Range*
I	Main beam	Main beam	I_{mm}
II	Main beam	Side-lobes	I_{ms}
III	Side-lobes	Main beam	I_{sm}
IV	Side-lobes	Side-lobes	I_{ss}

It is more complicated to derive the interference range I for DIR-Nets due to the directivity of antennas. In particular, we

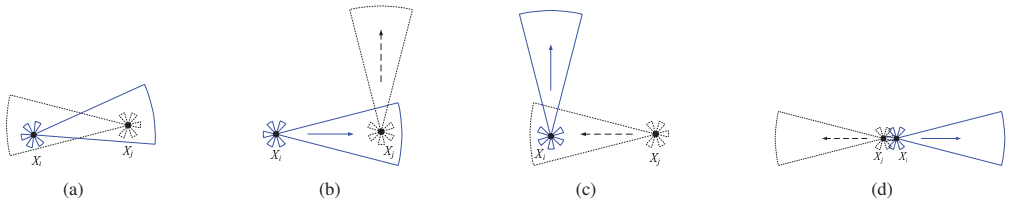

Fig. 3. Four scenarios: (**a**) Scenario (I), (**b**) Scenario (II), (**c**) Scenario (III), (**d**) Scenario (IV).

categorize our analysis into four different scenarios as shown in Table I.

In Scenario I, two nodes X_i and X_j interfere with each other if and only if they fall into the interference range of each other and their main antenna beams are pointed toward each other, as shown in Figure 3(a). In this case, the interference range denoted by I_{mm} can be calculated by

$$I_{mm} = \left(\frac{C_1 G_m G_m P}{P_0}\right)^{\frac{1}{\alpha}}, \tag{14}$$

where we replace both G_t and G_r in Equation (13) by G_m.

In Scenario II, the main antenna beam of the interfering node X_i is pointed to the interfered node X_j, which also falls into the interference range of X_i. However, the main beam of the interfered node X_j is not necessarily pointed to the interfering node X_i. Due to the existence of the side-lobes and the back-lobes, the reception of node X_j is interfered by node X_i, as shown Figure 3(b). Thus, the interference range denoted by I_{ms} can be calculated by

$$I_{ms} = \left(\frac{C_1 G_m G_s P}{P_0}\right)^{\frac{1}{\alpha}}, \tag{15}$$

where we replace G_t and G_r in Equation (13) by G_m and G_s, respectively.

Similar to Scenario II, the interference range in Scenario III, which is denoted by I_{sm}, can be calculated by

$$I_{sm} = \left(\frac{C_1 G_s G_m P}{P_0}\right)^{\frac{1}{\alpha}}, \tag{16}$$

where we replace G_t and G_r in Equation (13) by G_s and G_m, respectively.

It is obvious that $I_{ms} = I_{sm}$. Thus, we regard I_{ms} as I_{sm} interchangeably throughout the remaining paper.

In Scenario IV, the side-/back-lobes of the interfering node X_i and the interfered node X_j cover each other. Thus, we can calculate the interference range denoted by I_{ss}

$$I_{ss} = \left(\frac{C_1 G_s G_s P}{P_0}\right)^{\frac{1}{\alpha}}, \tag{17}$$

where we replace both G_t and G_r in Equation (13) by G_s.

C. Definitions

In this paper, we assume that there are n nodes in a plane and each node has only one antenna , which allows only one transmission or reception at a time. We also assume that each node is equipped with an identical antenna with the same beamwidth θ_m. Each node also has the same *transmission range* R_t and the same *interference range* I. Typically, I is no less than R_t, i.e. $I \geq R_t$.

We then have the following definitions.

Definition 1: Link Set. A link set is defined as a set of links among which no two links in this set share common nodes. Such a link set is denoted as LS. A link set is used to describe a set of links that need to act simultaneously.

Definition 2: Valid Assignment. A valid assignment to a link set is an assignment of channels such that no two conflicting links are assigned an identical channel. A link set is called a *Schedulable Link Set* if and only if there exists a valid assignment for the link set.

Definition 3: Node Density. There are n nodes randomly located in the plane. Let S denote the (infinite) set of sectors on the plane with interference range I and angle θ_m. The number of nodes within sector s is denoted as $N(s)$. The density of nodes is defined as $D = \max_{s \in S} N(s)$.
Note that we define

Then we give the definition of the upper bound on the number of channels to ensure collision-free communications in DIR-Nets.

Definition 4: Upper Bound on the number of channels. There exist possibly many valid link sets, which represent different combination of communication pairs among the nodes. The problem is to find a number, denoted as U, such that any link set LS derived from n nodes is schedulable using U channels. In other word, U is the upper bound of channels needed to ensure a collision-free link assignment.

The link assignment problem can be converted to a *conflict graph* problem, which is first addressed in [19]. A conflict graph is used to model the effects of interference.

Definition 5: Conflict Graph. We define a graph in which every link from a link set LS can be represented by a vertex. Two vertices in the graph are connected by an edge if and only if the two links conflict. Such a graph is called a conflict graph. The conflict graph G constructed from link set LS is denoted as $G(LS)$.

IV. Upper Bounds on the Number of Channels

A. Background Results

By constructing the conflict graph for a link set, and representing each channel by a different color, we found that the requirement that no two conflicting links share the same channel is equivalent to the constraint that no two adjacent vertices share the same color in graph coloring. Therefore, the problem of channel assignment on a link set can be converted

to the classical vertex coloring problem (in graph theory, the vertex coloring problem is a way of assigning "colors" to vertices of a graph such that no two adjacent vertices share the same color) on the conflict graph. The vertex coloring problem, as one of the most fundamental problems in graph theory, is known to be NP-hard even in the very restricted classes of planar graphs [20]. A coloring is regarded as valid if no two adjacent vertices use the same color.

The minimum number for a valid coloring of vertices in a graph G is denoted by a *chromatic* number, $\chi(G)$. There are two well-known results on the upper bound of $\chi(G)$, which will be used to derive our results.

Lemma 1: [21] If $\Delta(G)$ denotes the largest degree among G's vertices, *i.e.*, $\Delta(G) = \max_{v \in G} Degree(v)$, then we have

$$\chi(G) \leq \Delta(G) + 1$$

■

B. Upper Bounds on the Number of Channels

Before the derivation of upper bounds on the number of channels in DIR-Nets, we have the follow lemma to analyze the interference range I according to the aforementioned scenarios in Section III-A.

Lemma 2: When the main beamwidth θ_m is narrow, we have $I_{ss} \ll I_{ms} \ll I_{mm}$.

Proof. First, we have

$$\frac{I_{ss}}{I_{ms}} = \frac{(\frac{C_1 G_s G_s P}{P_0})^{\frac{1}{\alpha}}}{(\frac{C_1 G_m G_s P}{P_0})^{\frac{1}{\alpha}}} = (\frac{G_s}{G_m})^{\frac{1}{\alpha}}. \tag{18}$$

Similarly, we have

$$\frac{I_{ms}}{I_{mm}} = (\frac{G_s}{G_m})^{\frac{1}{\alpha}} \tag{19}$$

As shown in Eq. (8) and Eq. (9), when the beamwidth θ_m is narrow (e.g., $\theta_m \leq 10°$), $G_s \ll G_m$. Since the path loss factor α usually ranges from 2 to 5, it is obvious that $I_{ss} \ll I_{ms} \ll I_{mm}$. ■

We then derive the upper bounds on the number of channels to ensure collision-free communications in DIR-Nets with Sector antenna model.

Theorem 1: If there are n nodes in a planar area with the density D and each node is equipped with a directional antenna, for any valid link set LS derived from the n nodes, the corresponding conflict graph $G(LS)$ can be colored by using $2D + \frac{2DM\omega}{\theta_m} \cdot \left(\frac{G_s}{G_m}\right)^{\frac{2}{\alpha}} - 1$ colors.

Proof. We first derive the results based on *Sector* model (as shown in Fig. 4).

Consider link l_{ij} that consists of nodes X_i and X_j, as shown in Fig. 4. The interference region is denoted as two sectors with radius I and angle θ_m (the gray area in Fig. 4). From the definition of node density, each sector has at most D nodes. Other than nodes X_i and X_j, there are at most $D-1$ nodes in either sector. After we combine the nodes in the two sectors, the gray area contains no more than $2D-2$ nodes excluding nodes X_i and X_j.

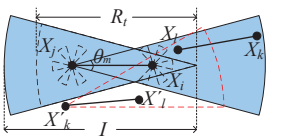

Fig. 4. Side/back-lobes included in interference region

Suppose link l_{kl} is one of the links that conflicts with l_{ij}. It is obvious that at least one node of that link, e.g., X_k, should be in X_j's interference region, the gray sector centered at X_j in Fig. 4. At the same time, the antenna of X_k should be pointed to X_j if it can interfere with X_j. Thus, X_k's interference region must also cover X_j. So, $|X_k - X_j| \leq I$. Since the antenna beam of the other node X_l should be turned toward X_k, it must also fall in the interference region of X_j, as shown in Fig. 4. Hence, $|X_l - X_j| \leq I$.

It seems that any link that conflicts with link l_{ij} must fall in the gray area representing the interference regions of nodes X_i and X_j. However, consider the case that X'_k and X'_l form a link l'_{kl} in Fig. 4. X'_l is outside the gray region of l_{ij}, but X'_k can interfere with X_i since its beam covers X_i. So, a link conflicting with link l_{ij} must contain at least one node falling in the gray area. Therefore, there are at most $2D-2$ links that conflict with l_{ij}.

We then extend the proof with consideration of side/back-lobes that are not completely covered by interference region as shown in Fig. 5. We denote the distance between X_i and X_j by d. To ensure that X_i can communicate with X_j, we require $d \leq R_t$, where R_t is the transmission range of X_i. The area of the interference region (including the interference region of the main beam as well as the interference region of the side-/back-lobes) varies with the different distance d. However, d cannot be too large, otherwise X_i and X_j cannot communicate with each other. It holds that $d \leq R_t$. When $d = R_t$, the analysis is the same as the above sector case. So, we omit the detailed analysis here.

When the distance d is decreased, the interference region caused by the side-/back-lobes may not be totally covered by the interference region of the main beam. For example, when d becomes much more smaller than R_t, as shown in Fig. 5, where the side-lobes and back-lobes, which cannot be totally covered by the interference region of the main lobes. In this case, the interference region has the maximum coverage area.

We then calculate the number of nodes in this interference region. The number of nodes falling into the side-lobe area is bounded $2 \cdot \frac{D}{\frac{\theta_m}{2} \cdot I_{mm}^2} \cdot M \cdot \omega \cdot I_{ss}^2 = \frac{2DM\omega}{\theta_m} \cdot \left(\frac{G_s}{G_m}\right)^{\frac{2}{\alpha}}$. Hence, the maximum degree of the vertices of G is $\Delta(G) \leq 2D + \frac{2DM\omega}{\theta_m} \cdot \left(\frac{G_s}{G_m}\right)^{\frac{2}{\alpha}} - 2$. From Lemma 1, the conflict graph can be colored by using $2D + \frac{2DM\omega}{\theta_m} \cdot \left(\frac{G_s}{G_m}\right)^{\frac{2}{\alpha}} - 1$ colors. ■

C. Discussions and implications

From the results, we found that the number of channels to ensure collision-free communications in DIR-Nets heavily depends on (i) the node density D and (ii) the antenna model (i.e., θ_m, ω and M). In particular, our results indicate that the

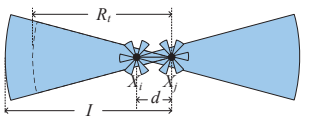

Fig. 5. Side/back-lobes not completely included in interference region.

higher node density results the more number of channels to ensure collision-free communications. Our findings imply that in the next generation wireless communication systems (e.g., 5G cellular networks), the fined-grained channel allocation mechanisms shall be designed, which however causes the new research challenges [22].

Besides, directional antennas have higher spectrum reuse than omni-directional antennas. One evidence is that the node density of OMN-Nets is larger than that of DIR-Nets as indicated in [5], [12]. Thus, if there are only limited channels available in a network, we can use directional antennas to cater for the collision-free transmission. In millimeter wave (mmWave) communication networks (i.e., potential solutions to 5G communication systems) [23], in order to overcome the high attenuation of mmWave radio signal (the radio frequency is above 30GHz), directional antennas are compulsorily equipped with wireless devices. One of research issues in such mmWave networks is how to assign channels to improve the spectrum reuse. Our study in this paper offers a solution to such new challenge.

V. Conclusions

How to efficiently use the radio spectrum has received extensive attentions recently. Some of previous works concerned with using multiple channels in wireless network with omni-directional antennas. The performance improvement is limited due to the broadcasting features of omni-directional antennas, which have high interference. There are other works considering wireless networks with directional antennas, which concentrate the transmission to some desired directions and consequently improve the network performance. But, there are few studies on integrating directional antennas with multiple channels together. This paper is one of pioneer works in the new area. In particular, we establish an analytical model to analyze the maximum number of channels to ensure the collision-free communications in DIR-Nets. More specifically, we propose a novel antenna model - Iris to completely depict the features of realistic antennas. On one hand, this model depicts directional antennas more accurately than other existing simple antenna models. On the other hand, this model is more general since other existing models can be regarded as special cases of our Iris model. Besides, our theoretical results also offer many useful insights to design wireless networks.

Acknowledgement

The work described in this paper was partially supported by Macao Science and Technology Development Fund under Grant No. 096/2013/A3 and the NSFC-Guangdong Joint Fund under Grant No. U1401251. The authors would like to thank Gordon K.-T. Hon for his constructive comments.

References

[1] P. Bahl, R. Chandra, and J. Dunagan, "SSCH: Slotted seeded channel hopping for capacity improvement in ieee 802.11 ad-hoc wireless networks," in *Proceedings of Mobicom*, 2004.

[2] R. Draves, J. Padhye, and B. Zill, "Routing in multi-radio, multi-hop wireless mesh networks," in *Proceedings of Mobicom*, 2004.

[3] M. Kodialam and T. Nandagopal, "Characterizing the capacity region in multi-radio multi-channel wireless mesh networks," in *Proceedings of MobiCom*, 2005.

[4] P. Kyasanur and N. H. Vaidya, "Capacity of multichannel wireless networks: Impact of number of channels and interfaces," in *Proceedings of MobiCom*, 2005.

[5] L. Cao and M.-Y. Wu, "Upper bound of the number of channels for conflict-free communication in multi-channel wireless networks," in *Proceedings of IEEE WCNC*, 2007.

[6] P. Li, C. Zhang, and Y. Fang, "The Capacity of Wireless Ad Hoc Networks Using Directional Antennas," *IEEE Transactions on Mobile Computing*, vol. 10, no. 10, pp. 1374–1387, 2011.

[7] J. Zhang and S. C. Liew, "Capacity improvement of wireless ad hoc networks with directional antennae," *Mobile Computing and Communications Review*, vol. 10, no. 4, pp. 17–19, 2006.

[8] H.-N. Dai, K.-W. Ng, and M.-Y. Wu, "On collision-tolerant transmission with directional antennas," in *Proceedings of IEEE WCNC*, 2008.

[9] ——, "On busy-tone based MAC protocol for wireless networks with directional antennas," *Wireless Personal Communications*, vol. 73, no. 3, pp. 611 – 636, 2013.

[10] H.-N. Dai, K.-W. Ng, R. C.-W. Wong, and M.-Y. Wu, "On the Capacity of Multi-Channel Wireless Networks Using Directional Antennas," in *Proceedings of IEEE INFOCOM*, 2008.

[11] H. Xu, H.-N. Dai, and Q. Zhao, "On the connectivity of wireless networks with multiple directional antennas," in *the 18th IEEE International Conference on Networks (ICON)*, 2012.

[12] H.-N. Dai, K.-W. Ng, and M.-Y. Wu, "Upper bounds on the number of channels to ensure collision-free communications in multi-channel wireless networks using directional antennas," in *Proceedings of IEEE WCNC*, 2010.

[13] C. A. Balanis, *Antenna Theory : Analysis and Design*, 3rd ed. New York: John Wiley & Sons, 2005.

[14] M. Kiese, C. Hartmann, and R. Vilzmann, "Optimality bounds of the connectivity of adhoc networks with beamforming antennas," in *IEEE GLOBECOM*, 2009.

[15] R. Ramanathan, "On the performance of ad hoc networks with beamforming antennas," in *Proceedings of MobiHoc*, 2001.

[16] S. Yi, Y. Pei, and S. Kalyanaraman, "On the capacity improvement of ad hoc wireless networks using directional antennas," in *Proceedings of ACM MobiHoc*, 2003.

[17] R. Ramanathan, J. Redi, C. Santivanez, D. Wiggins, and S. Polit, "Ad hoc networking with directional antennas: A complete system solution," *IEEE JSAC*, vol. 23, no. 3, pp. 496–506, 2005.

[18] T. S. Rappaport, *Wireless communications : principles and practice*, 2nd ed. Upper Saddle River, N.J.: Prentice Hall PTR, 2002.

[19] K. Jain, J. Padhye, V. N. Padmanabhan, and L. Qiu, "Impact of interference on multi-hop wireless network performance," in *Proceedings of ACM MobiCom*, 2003.

[20] D. B. West, *Introduction to graph theory*, 2nd ed. Upper Saddle River, N.J.: Prentice Hall PTR, 2001.

[21] A. Panconesi and R. Rizzi, "Some simple distributed algorithms for sparse networks," *Distributed Computing*, vol. 14, no. 2, pp. 97–100, 2001.

[22] T. Wang, Y. Sun, L. Song, and Z. Han, "Social data offloading in d2d-enhanced cellular networks by network formation games," *IEEE Transactions on Wireless Communications*, vol. 14, no. 12, pp. 7004–7015, 2015.

[23] J. Qiao, X. Shen, J. W. Mark, Q. Shen, Y. He, and L. Lei, "Enabling device-to-device communications in millimeter-wave 5g cellular networks," *IEEE Communications Magazine*, vol. 53, no. 1, pp. 209–215, January 2015.